# LINEAR INVERSE APPROACHES FOR THE RECONSTRUCTION OF EPICARDIAL AND TRANSMEMBRANE POTENTIAL PATTERNS

B. Messnarz[1], B. Tilg[1], R. Modre[1], G. Fischer[1,2], F. Hanser[1], P. Wach[1]
[1]Institute of Biomedical Engineering, Graz University of Technology, Graz, Austria
[2]Clinical Department of Cardiology, University Hospital Innsbruck, Innsbruck, Austria

*Abstract*-**In this study we compare two different linear inverse approaches to the inverse problem of electrocardiography. Method A is the standard Tikhonov zero order approach used as a reference method. Method B is based on the general deconvolution theorem proposed by Greensite. Both methods are applied to both the epicardial potential and the transmembrane potential considered as the primary source. In order to compare the performance of both methods the activation time pattern is estimated.**

***Keywords* - Inverse problem of electrocardiography, transmembrane potential, epicardial potential, ill-posed problems**

## I. INTRODUCTION

Noninvasive functional imaging of the electrical sources of the human heart is enabled by electrocardiographic (ECG) mapping in combination with magnetic resonance imaging (MRI). According to the bidomain theory [8] the transmembrane potential $\varphi_m$ is considered the primary electrical source in the human heart. Due to admissible assumption of electrical isotropy of the myocardium during the depolarization [2, 8] the corresponding forward problem degenerates to a two-dimensional field and scalar potential problem. The connection between the transmembrane potential and the potential on all conductivity interfaces as well as the body surface potential (BSP) is given by a Fredholm integral equation of second kind (Geselowitz equation). In general, the boundary element method [1, 2] (BEM) is employed for solving this kind of problem numerically which yields to an ill-posed and rank-deficient system of linear equations. For the inverse problem regularization techniques are required to estimate parameters describing features of $\varphi_m$ (e.g. the activation time (AT) defined as the onset of $\varphi_m$) or the epicardial potential $\varphi_e$. An empirical way to estimate the AT from the epicardial potential is presented in [6]. The standard regularization method is referred to as Tikhonov zero order regularization (method A in this study). A different and novel method used in this study was proposed by Greensite [3] (method B).

AT imaging methods are of great clinical interest. These methods enable the spatially resolved reconstruction of single focal, multiple focal and more complicated activation patterns. Non-invasive imaging of ectopic and pre-excited ventricular activation may be one of the possible clinical applications.

## II. MATHEMATICAL METHODS

In order to discretize the Geselowitz equation in the volume bounded by the heart surface and the torso surface the BEM was applied to result in the following matrix equation, when the transmembrane potential is considered the source:

$$\mathbf{D} = \mathbf{L}_m \mathbf{\Phi}_m \tag{1}$$

where $\mathbf{D}$ is the ECG data matrix with column vectors $\mathbf{d}_t$ representing an ECG map for one certain time instant $t$, $\mathbf{L}_m$ is the lead-field or transfer matrix for the transmembrane potential and $\mathbf{\Phi}_m$ is the discrete transmembrane potential. The column vectors of $\mathbf{\Phi}_m$, denoted by $\boldsymbol{\varphi}_m$, are the transmembrane potential distribution on the heart surface at the time instant corresponding to the column index.

When the epicardial potential is the favoured quantity to reconstruct one has in principal to solve Laplace's equation in the volume between the epicardial surface and the torso surface. Applying the BEM yields to a similar equation for the connection between the epicardial potential and the BSP:

$$\mathbf{D} = \mathbf{L}_e \mathbf{\Phi}_e \tag{2}$$

where $\mathbf{L}_e$ is the lead-field matrix for the discrete epicardial potential $\mathbf{\Phi}_e$.

Because of the ill-posed nature of the inverse problem, we cannot simply invert (1) or (2) to compute $\boldsymbol{\varphi}_m$ or $\boldsymbol{\varphi}_e$. Regularization schemes which incorporate further temporal and spatial information are necessary. In the following section of regularization techniques we do not distinguish formally between the epicardial and transmembrane potential settings. So $\mathbf{L}$ denotes the lead-field matrix an $\boldsymbol{\varphi}$ the corresponding epicardial or transmembrane potential.

*Method A: Standard zero order Tikhonov regularization*

For each fixed value of $t$ in $T$ ($T$ means the time interval during the QRS-complex over which the ECG-data are collected), (1) and (2) reduce to

$$\mathbf{d}_t = \mathbf{L}\boldsymbol{\varphi}_t \tag{3}$$

We obtain a regularized solution to (3) by minimizing the following objective function:

$$\left\|\mathbf{L}\boldsymbol{\varphi}_t - \mathbf{d}_t\right\|_2^2 + \lambda^2(t)\left\|\boldsymbol{\varphi}_t\right\|_2^2 \rightarrow \min \tag{4}$$

with the so-called regularization parameter $\lambda$. The first term in (4) represents the least-square solution of (3) while the second term is the regularization term that constrains the norm of the solution (in case of Tikhonov zero order). Performing the singular value decomposition (SVD) of $\mathbf{L}$,

$$\mathbf{L} = \mathbf{U}\mathbf{\Sigma}\mathbf{V}^T, \tag{5}$$

we can write the solution of (3) as

$$\boldsymbol{\varphi}_t = \sum_i \frac{\lambda(t)^2}{\lambda(t)^2 + \sigma_i^2}\left(\mathbf{u}_i{}^T \mathbf{d}_t\right)\mathbf{v}_i \tag{6}$$

were $\mathbf{u}_i$ and $\mathbf{v}_i$ are the column vectors of the matrices $\mathbf{U}$ and $\mathbf{V}$ and $\sigma_i$ are the singular values (the main-diagonal elements of $\mathbf{\Sigma}$). A crucial point is the choice of the optimal regularization parameter $\lambda$ which controls the degree of smoothing. Several methods for regularization parameter choice are established in literature. In this study $\lambda$ is determined by the L-curve criterion [5]. This method involves a parametric log-log scale

# Report Documentation Page

| Report Date | Report Type | Dates Covered (from... to) |
|---|---|---|
| 25OCT2001 | N/A | - |

| | |
|---|---|
| **Title and Subtitle**<br>Linear Approaches for the Reconstruction of Epicardial and Transmembrane Potential Patterns | **Contract Number** |
| | **Grant Number** |
| | **Program Element Number** |
| **Author(s)** | **Project Number** |
| | **Task Number** |
| | **Work Unit Number** |
| **Performing Organization Name(s) and Address(es)**<br>Institute of Biomedical Engineering, Graz University of Technology, Graz, Austria | **Performing Organization Report Number** |
| **Sponsoring/Monitoring Agency Name(s) and Address(es)**<br>US Army Research, Development & Standardization Group (UK) PSC 802 Box 15 FPO AE 09499-1500 | **Sponsor/Monitor's Acronym(s)** |
| | **Sponsor/Monitor's Report Number(s)** |

**Distribution/Availability Statement**
Approved for public release, distribution unlimited

**Supplementary Notes**
Papers from the 23rd Annual International Conference of the IEEE Engineering in Medicine and Biology Society, 25-28 October 2001, held in Istanbul, Turkey. See also ADM001351 for entire conference on cd-rom., The original document contains color images.

**Abstract**

**Subject Terms**

| | |
|---|---|
| **Report Classification**<br>unclassified | **Classification of this page**<br>unclassified |
| **Classification of Abstract**<br>unclassified | **Limitation of Abstract**<br>UU |

**Number of Pages**
4

plot of the solution norm $\|\boldsymbol{\varphi}_t\|$ on the ordinate against the residual norm $\|\mathbf{L}\boldsymbol{\varphi}_t - \boldsymbol{d}_t\|$ on the abscissa with $\lambda$ as parameter. This so-called L-curve is plotted for each point of time. The optimal $\lambda$ is characterized by the corner of the L-curve, i.e. the point of the maximum curvature. We emphasize that $\lambda$ is computed for each time instant separately, hence it becomes time dependent.

*Method B: improved method*

Greensite [3] proposed a new method for regularizing the ill-posed problem of computing epicardial potentials from the body surface potentials. This method can also be utilized to compute transmembrane potentials. The main difference to ordinary Tikhonov scheme is that this method simultaneously regularizes equations associated with all time points. In the following this will become clearer. Write the SVD of the data matrix as

$$\mathbf{D} = \mathbf{PQR}^T , \tag{7}$$

where **P** is the matrix of basis vectors according to the spatial domain of the data, **Q** is a diagonal matrix with the singular values as its diagonal elements and **R** is the matrix of basis vectors spanning the time domain of the data. The original equation transforms now to

$$\mathbf{L\Phi} = \mathbf{PQR}^T . \tag{8}$$

Multiplying (8) by **R** and using the relation $\mathbf{R}^T\boldsymbol{R}=\mathbf{I}$ yields to

$$\mathbf{L\Phi R} = \mathbf{PQ} . \tag{9}$$

Let us denote the matrix **ΦR** by **X** and write the above equation for each column of **X** and **PQ**:

$$\mathbf{L}\mathbf{x}_i = q_i\mathbf{p}_i . \tag{10}$$

Recall that the $\mathbf{p}_i$ are the basis vectors according to the spatial domain of the data. In [3] it is proved that more accurate results are achieved by regularizing (10), i .e. to find the inverse solution for the $\mathbf{x}_i$ which represent the sources for the $\mathbf{p}_i$. Using the Tikhonov scheme we obtain the inverse solution

$$\mathbf{x}_i = \sum_i \frac{\lambda^2}{\lambda^2 + \sigma_i^2}\left(\mathbf{u}_i{}^T q_i\mathbf{p}_i\right)\mathbf{v}_i . \tag{11}$$

We reconstruct only equations of (10) satisfying the discrete Picard condition [4] while the other remaining equations are eliminated (interequation truncation). The regularization parameter is again determined by the L-curve criterion. By multiplying the reconstructed matrix **X** by $\mathbf{R}^T$ we obtain the desired potential:

$$\mathbf{\Phi} = \mathbf{XR}^T \tag{12}$$

*Activation Time*

In order to compare the performance of both methods we compute the AT on the epicardial surface. For the transmembrane potential it is obvious to define the AT as time of the first time derivative's maximum of the reconstructed transmembrane potential evolution. In case of the epicardial potential we refer to the empirical method presented in [6]. Therein the AT is obtained by determining the time of occurrence of the negative peak of the first time derivative of the potential at each source point.

## III. RESULTS

Our simulations were accomplished with synthetic ECG-data with a realistic heart and torso model. The MRI of the torso and heart anatomy was generated under clinical conditions. To this end, the torso of a 21-year old male patient was imaged with a 1.5 Tesla MR scanner (Siemens Vision Plus). In order to shape the surface of the heart, the cardiac muscle was imaged in an ECG-gated breath-hold oblique imaging mode. Fig. 1. shows the torso anatomy with two axial MRI scans, the modeled chest surface, the lungs' surfaces and the model of the ventricular surface from a left-lateral oblique view.

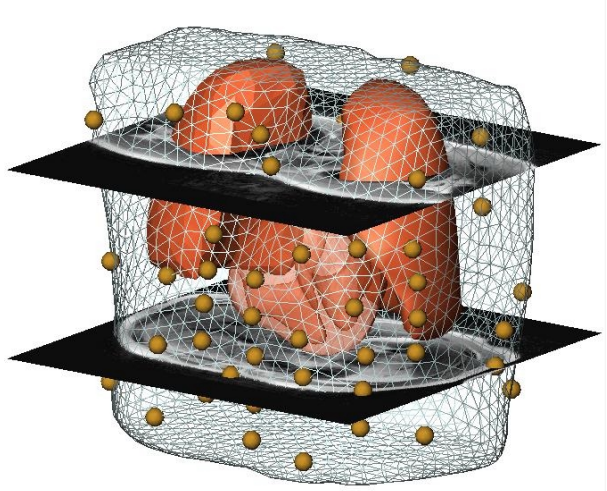

Fig.1. Torso model generated from 3D MRI data with two axial MR scans from a left-lateral oblique view. Both lungs and the ventricular surface are depicted too. The spheres represent the electrode positions.

The epicardial potential-to-BSP as well as the transmembrane potential-to-BSP transfer matrix were computed as solution to the "forward problem". The triangular mesh for the epicardial surface consisted of 422 nodes.

Synthetic BSP-data at 42 electrode locations at the torso's surface were calculated utilizing the forward model. For this purpose a reference AT map was estimated by a reference inverse method [7] applied to measured BSP data. This data was acquired under clinical conditions and reflect a cardiac rhythm resulting from catheter pacing in the apex of the right ventricle. The reference AT map is shown in Fig. 2. from an anterior epicardial view. Gaussian noise was added to the synthetic BSP data for signal-to-noise ratio of 30 dB. The time points are taken at 1ms time increments to encompass a 135ms interval containing the activation (QRS) interval.

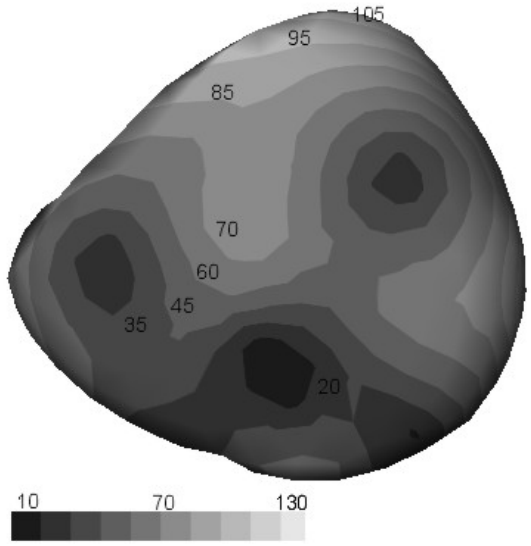


Fig.2. Reference AT map on the anterior epicardium in ms estimated from measured data by the method presented in [7]. The pattern shows more distributed events including one early breakthrough near the apex and two early activation events on left and right lateral site of the anterior epicardium.

For inverse method A the regularization parameter $\lambda$ was determined at 135 time points by the L-curve criterion (maximum curvature). We experienced that slightly smoothing of the temporal $\lambda$-trend by cubic splines leads to better results for the inverse solution, in fact, reflected by an improvement of the correlation coefficient for the AT map from 0.77 (non smoothed) up to 0.91 (smoothed). The reconstructed AT maps are depictured in Fig. 3. The upper panel shows the AT result for the anterior epicardium calculated in the setting for the epicardial potential. In order to estimate the AT from the reconstructed epicardial potential the first time derivative had to be determined. The numerically computing of the time derivative was enabled by smoothing with cubic spline interpolation. A correlation coefficient of 0.91 and a relative error of 0.16 could be attained. (Relative error is the square-root of the sum of the squares of the difference between reference and computed AT divided by the square-root of the sum of the squares of the reference AT, where the sums are over all source points of the epicardial surface). In comparison the lower panel of Fig. 3 reflects the results of the transmembrane potential setting. A similar procedure for AT computing yielded to values of 0.88 and 0.17 for the correlation coefficient and the relative error, respectively. In view of both results we can not state essential differences using the epicardial potential formalism and the transmembrane potential formalism. The main characteristics of the reference AT pattern could be retrieved in both approaches.

For inverse method B equation sequence (10) constitutes 42 equations (i=1, … ,42) according to 42 basis vectors $\mathbf{p}_i$ of the spatial domain on the electrodes site. As mentioned before it is meaningful to solve the $m$th equation only if the discrete Picard condition is satisfied. Thus, for the first 8 equations the

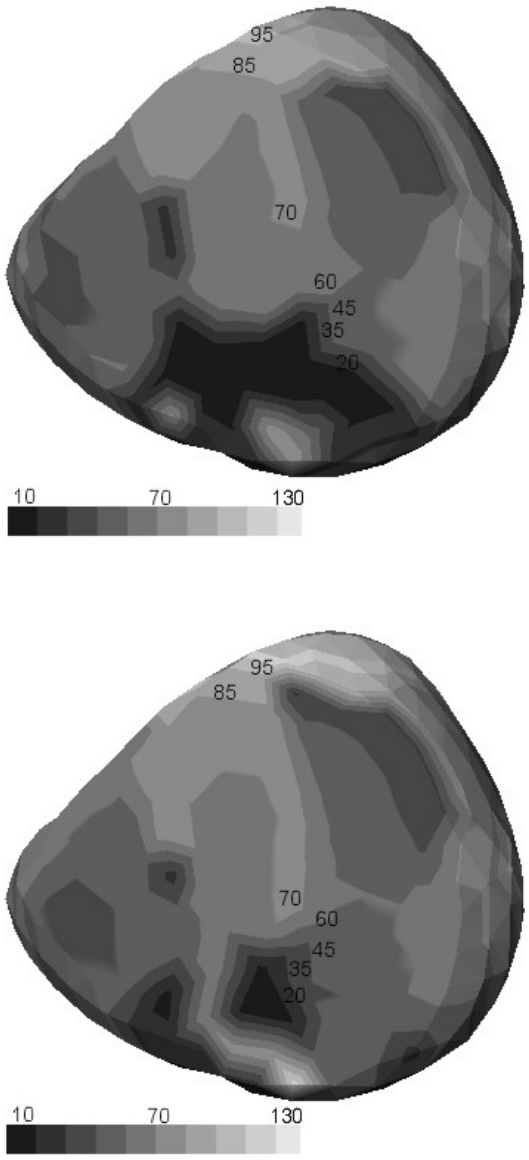


Fig.3. Reconstructed AT map on the anterior epicardium applying inverse method A. The upper panel shows the solution based on the epicardial setting in comparison to the lower panel, where the transmembrane potential represents the source.

solution was obtained by (11) calculating the suited regularization parameter by the L-curve criterion. The results for the AT are presented in Fig. 4. In the upper panel the estimated AT in the epicardial potential setting is illustrated The corresponding correlation coefficient is disposed to 0.90 and for the relative error a value of 0.17 was obtained. In addition, the result of the transmembrane potential formulation is shown in the lower panel. Similar values of 0.91 and 0.17 for the correlation coefficient and the relative error, respectively, can be found. Again, no substantial varieties in both, the epicardial and transmembrane potential setting can be seen from Fig. 4. Both display the main events of the reference pattern in an acceptable way. However, in contrast

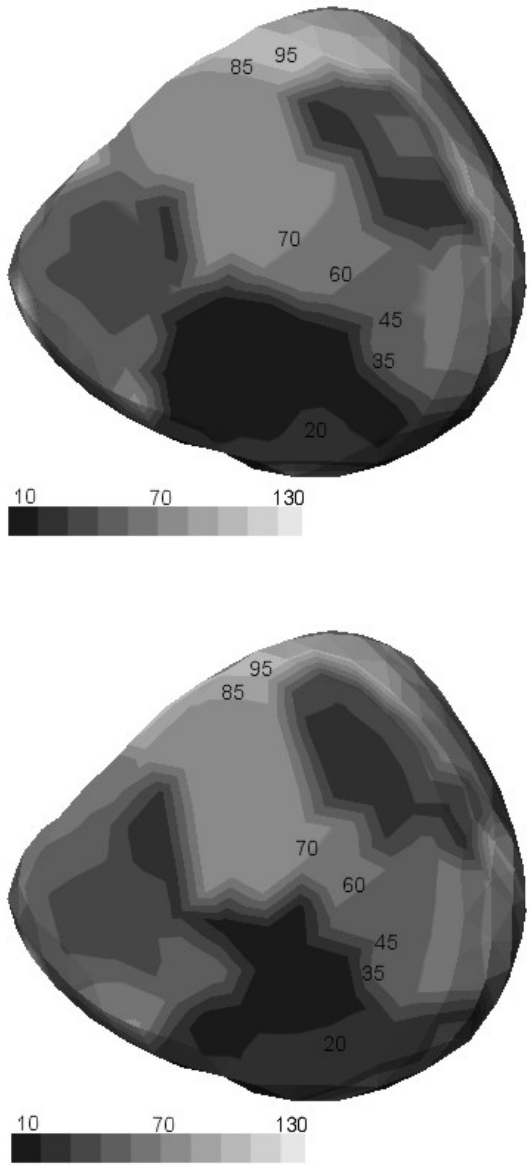


Fig.4. Reconstructed AT map on the anterior epicardium applying inverse method B. The upper panel shows the solution based on the epicardial setting in comparison to the lower panel, where the transmembrane potential represents the source.

to method A method B yields better results, which can be seen, in particular, by smoother AT patterns.

## IV. Discussion and Conclusions

The reconstruction of epicardial potentials from the BSP constitutes the standard approach to the electrocardiographic inverse problem. To provide the cardiologist with information of clinical interest (e.g., the AT), however, one has to solve another inverse problem or to utilize some empirical methods as done in this study. Furthermore, no information regarding the endocardium can be extracted with the epicardial setting. To overcome this drawback one can employ the transmembrane potential formalism which allows to reconstruct source patterns on the epicardium and on the endocardium as well. On the epicardium both settings lead to similar results as shown in this study. The transmembrane potential formalism, however, enables more powerful regularization methods, because more physiological a-priori information can be imposed on the sought solution. Therefore further research will be focused on the spatio-temporal regularization of the transmembrane potential inverse approach.

## Acknowledgment

This work was supported by the START Y144-INF program funded by the Federal Ministry of Education, Science and Culture, Vienna, Austria.

## References

[1] G. Fischer, B. Tilg, P. Wach, R. Modre, U. Leder, H. Nowak, "Application of high-order boundary elements to the electrocardiographic inverse problem*," Comput. Meth. Prog. Biomed.*, vol. 58(2), pp. 119-131, 1999

[2] G. Fischer, B. Tilg, R. Modre, G.J.M. Huiskamp, J. Fetzer, W. Rucker, P. Wach, "A bidomain model based BEM-FEM formulation for anisotropic cardiac tissue," *Ann. Biomed. Eng.*, vol. 28, pp.1229-1243, 2000

[3] F. Greensite, "An improved method for estimating epicardial potentials from the body surface," *IEEE Trans. Biomed. Eng.,* vol. 45, pp. 98-104, 1998.

[4] P. C. Hansen, "Numerical tools for analysis and solution of Fredholm integral equation of first kind," *Inverse Problems,* vol. 8, pp. 849-872, 1992.

[5] P.C. Hansen, "Analysis of discrete ill-posed problems by means of the L-curve," *SIAM Rev.*, vol. 34, pp. 561-580, 1992

[6] D. S. Khoury, B. Taccardi, R. L. Lux, P. R. Ershler, Y. Rudy, "Reconstruction of endocardial potentials and activation sequences from intracavitary probe measurements - localization of pacing sites and effects of myocardial structure," *Circulation*, vol. 91, pp. 845-863, 1995.

[7] R. Modre, B. Tilg, G. Fischer, P. Wach, "An iterative algorithm for myocardial activation time imaging*," Comput. Meth. Prog. Biomed.*, vol. 64, pp. 1-7, 2001

[8] Y. Yamashita, D. Geselowitz, "Sourcefield relationships for cardiac generators on the heart surface based on their transfer coefficients," *IEEE Trans. Biomed. Eng.,* vol. 32, pp. 964-970, 1985.